Current Biology 19, 1925–1931, December 1, 2009 ©2009 Elsevier Ltd All rights reserved DOI 10.1016/j.cub.2009.09.022

Report

Convergent Evolution of Novel Protein Function in Shrew and Lizard Venom

Yael T. Aminetzach,[1] John R. Srouji,[2] Chung Yin Kong,[3] and Hopi E. Hoekstra[1,*]
[1]Department of Organismic and Evolutionary Biology and the Museum of Comparative Zoology
[2]Department of Molecular and Cellular Biology
Harvard University, Cambridge, MA 02138, USA
[3]Institute for Technology Assessment, Massachusetts General Hospital, Boston, MA 02114, USA

Summary

How do proteins evolve novel functions? To address this question, we are studying the evolution of a mammalian toxin, the serine protease BLTX [1], from the salivary glands of the North American shrew *Blarina brevicauda*. Here, we examine the molecular changes responsible for promoting BLTX toxicity. First, we show that regulatory loops surrounding the BLTX active site have evolved adaptively via acquisition of small insertions and subsequent accelerated sequence evolution. Second, these mutations introduce a novel chemical environment into the catalytic cleft of BLTX. Third, molecular-dynamic simulations show that the observed changes create a novel chemical and physical topology consistent with increased enzyme catalysis. Finally, we show that a toxic serine protease from the Mexican beaded lizard (GTX) [2] has evolved convergently through almost identical functional changes. Together, these results suggest that the evolution of toxicity might be predictable—arising via adaptive structural modification of analogous labile regulatory loops of an ancestral serine protease—and thus might aid in the identification of other toxic proteins.

Results and Discussion

How proteins evolve novel functions in nature remains largely unknown. One approach to addressing this question is to study molecular changes that result in functional convergence. Venom evolution provides an ideal system in which to study genetic novelty because in many cases the proteins involved in toxicity have been identified and have evolved independently across a variety of animals [3]. Here we first identify the molecular changes associated with the evolution of toxicity in a shrew and then document its remarkable functional convergence with a lizard venom.

Although venom has been well characterized in reptiles, toxicity has also evolved in a number of mammals, most often in insectivores of the order Soricomorpha—a venomous bite has been verified in solenodons [4], Eurasian water shrews [5], and the American short-tailed shrew (*Blarina brevicauda*) [6, 7]. The initial characterization of the serine protease BLTX from *B. brevicauda* [1] provided the first evidence for the biochemical basis of shrew toxicity. Subsequently, a nontoxic homolog, blarinasin-1, has been purified from *B. brevicauda* salivary glands [8], and the sequence of an uncharacterized homolog blarinasin-2 has been reported (Uniprot ID: Q5FBW1). All three proteins show the highest sequence similarity to mammalian glandular kallikrein-1 serine proteases [9] (e.g., BLTX, blarinasin-1, and blarinasin-2 are 55.5%, 54.1%, and 54.1% identical at the amino acid level to human kallikrein-1, respectively). Therefore the most recent common ancestor of BLTX, blarinasin-1, and blarinasin-2 is probably an ortholog of the kallikrein-1 gene.

Based on sequence comparisons of the three extant *B. brevicauda* genes, we reconstructed their evolutionary history: the duplication of the ancestral protein resulted in BLTX and the ancestor to blarinasin-1 and -2, followed by a more recent duplication yielding blarinasin-1 and -2, which share high sequence identity (98.2% at the amino acid level). Importantly, recent studies suggest that BLTX toxicity is due to an increase in catalytic activity relative to its nontoxic homologs, thereby flooding the circulatory system with the catalytic byproduct bradykinin, which in high doses can lead to paralysis and death [1, 2, 8]. Thus, the molecular changes required for toxicity have probably occurred along the BLTX lineage and are associated with an increase in enzyme activity.

Insertions in BLTX Regulatory Loops May Promote Toxicity

To identify changes that could contribute to the evolution of toxicity, we first examined sequence differences between BLTX and its nontoxic homologs. Using a combination of amino acid and nucleotide sequence alignments (see the Supplemental Data available online) with mammalian kallikrein-1 enzymes, we find two independent in-frame insertions of 21 bp (insert 1: L115-M121 in BLTX) and 12 bp each (insert 2: F125-K128) that flank a 9 bp conserved element present in all kallikrein-1 genes (Figure 1A). We also identified two additional in-frame insertions unique to *B. brevicauda*: a 9 bp element corresponding to residues N54-V56 (insert 3) and a 3 bp element (S179) present only in BLTX (insert 4; Figure 1A). Because these insertions are unique to *B. brevicauda* and shrews are nested well within the mammalian phylogeny (Figure 1A), all four insertions are probably derived in *B. brevicauda*.

To determine the functional significance, if any, of these insertions, we first examined their position in the enzyme. Intriguingly, all of these insertions occurred within three loops that surround the active site, which is defined as the cleft encompassing the conserved catalytic triad Asp-His-Ser [10] (Figure 1B). Two of the insertions (insert 1 and 2) are found in a well-characterized secondary structure (22 residues) termed the "kallikrein loop," [11] herein designated as loop 1. In kallikreins, this loop contacts the substrate peptide above the catalytic triad [10] and contributes to the enzyme's specificity and rate of catalysis [12, 13]. Moreover, variation within this region is thought to contribute to kallikrein functional diversity [13]—the 15 known human kallikrein paralogs differ in kallikrein loop length and amino acid composition, and this variation is thought to confer their distinct physiological roles [10]. The other two insertions are found in regions designated as loop 2 (8 residues) and loop 3 (11 residues) that also surround the catalytic triad (Figure 1B), and thus, they too are likely to

*Correspondence: hoekstra@oeb.harvard.edu

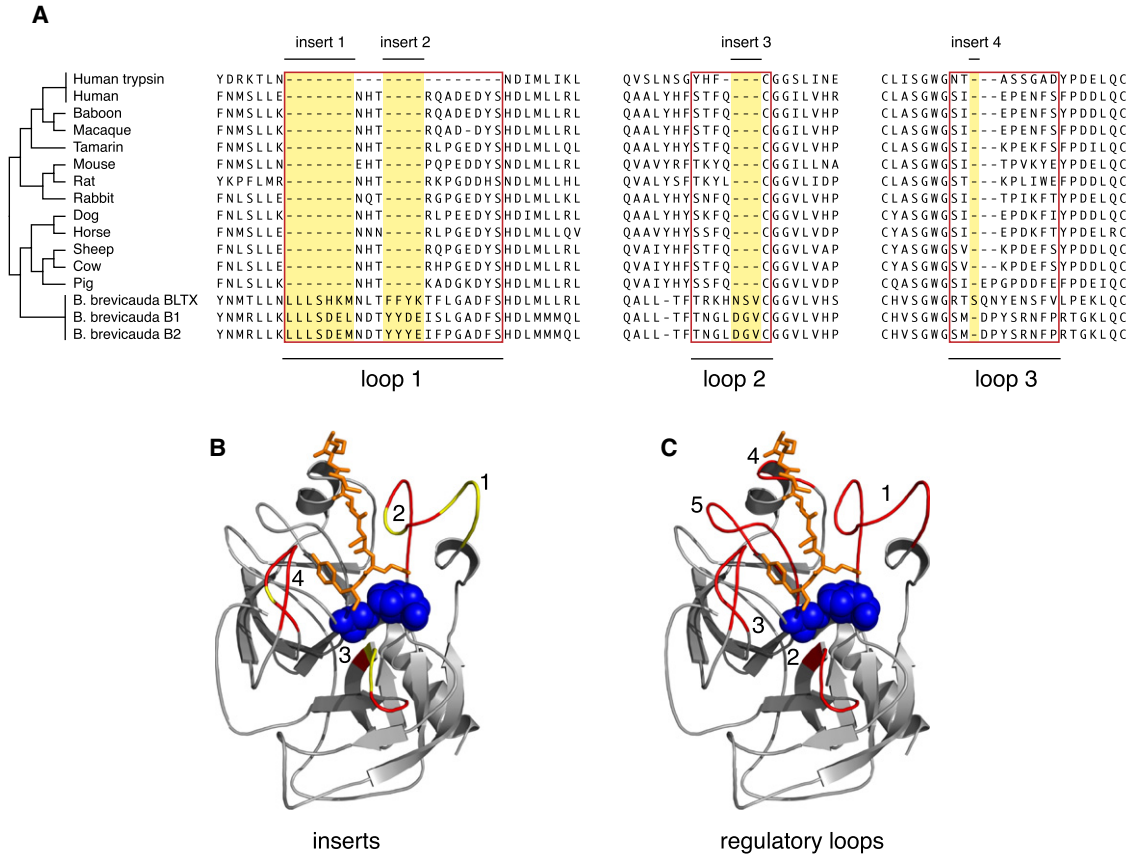

Figure 1. Multiple Small Insertions Unique to Shrew Kallikrein Regulatory Loops

(A) Amino acid sequence alignment of *Blarina brevicauda* BLTX, blarinasin-1 (B1), and blarinasin-2 (B2) with 12 other mammalian kallikrein-1 enzymes and human trypsin based on automated amino acid alignments and refined manually with nucleotide sequences (see Supplemental Data). Topology depicting species relationships shown on left (from [22]). Four insertions are highlighted (yellow) and all occur in the regulatory loops (red boxes) surrounding the active site.

(B) A 3D model of BLTX (constructed based on human kallikrein-3 structure, Protein Data Bank ID 2ZCK; [23]) shows insert position (yellow) in three (of five) regulatory loops (red) above the catalytic triad Asp-His-Ser (blue) in the active site. A substrate analog (fluorogenic oligopeptide Mu-KGISSQY-AFC; orange) is shown docked. Substrate is proximate to loop 1 (the kallikrein loop).

(C) The five regulatory loops (red), all of which experience positive selection, surround the active site.

regulate enzyme activity. However, because the nontoxic blarinasin-1 also contains the same insertions as BLTX (with the exception of insert 4 unique to BLTX), the presence of these insertions alone is not sufficient to confer toxicity.

BLTX Regulatory Loops Evolved under Positive Selection

It then follows that, in addition to insertions, other mutations may contribute to changes in theses regulatory loops and hence enzyme activity. To determine whether positive selection has acted on the loops, we tested for an excess of nonsynonymous mutations (Ka/Ks analysis) among BLTX, blarinasin-1, and blarinasin-2. When considering the entire protein sequence, we did not find a deviation from neutral expectations in any pairwise comparison (Table S1). Although this suggests that overall the protein is evolving under purifying selection, any localized signal would be obscured by averaging across regions [14]. Therefore, we performed a Ka/Ks analysis on three-dimensional (3D) structural regions (following [15]), defined based on a BLTX protein model. Specifically, we tested for positive selection on the region surrounding the active site, which comprises five loops (1–5, total of 61 residues; Figure 2A, Table S1) that are likely to affect substrate accessibility because of their proximity to the active site. This region includes loops 1–3, each containing an insertion unique to shrews. Together, these five loops show evidence for positive selection in a comparison between BLTX and blarinasin-1 ($Ka/Ks = 1.6$, $G = 15.4$, $p < 0.001$), and BLTX and blarinasin-2 ($Ka/Ks = 1.4$, $G = 15.1$, $p < 0.001$); analysis of each loop separately is statistically challenging because individual loops are short. Although BLTX and blarinasin-1 differ at only 32% of amino acid sites overall, we find that the five loops have changed nearly twice as much (62% across sites). Moreover, a substantial fraction of these amino acid changes occurred in the loop 1 and 2 insertions (7 of 10 and 2 of 5 sites, respectively). Other regions of the protein do not show elevated rates of sequence change (Table S1). The excess of derived amino-acid changes in BLTX's regulatory loops, many of which occur in the loop 1 and 2 insertions, suggests that both the insertions and the extensive sequence evolution in the regulatory loops might be important for toxicity.

Novel Physicochemical Properties of the Regulatory Loops

In addition to showing an excess of amino acid mutations in BLTX regulatory loops, we determined whether these

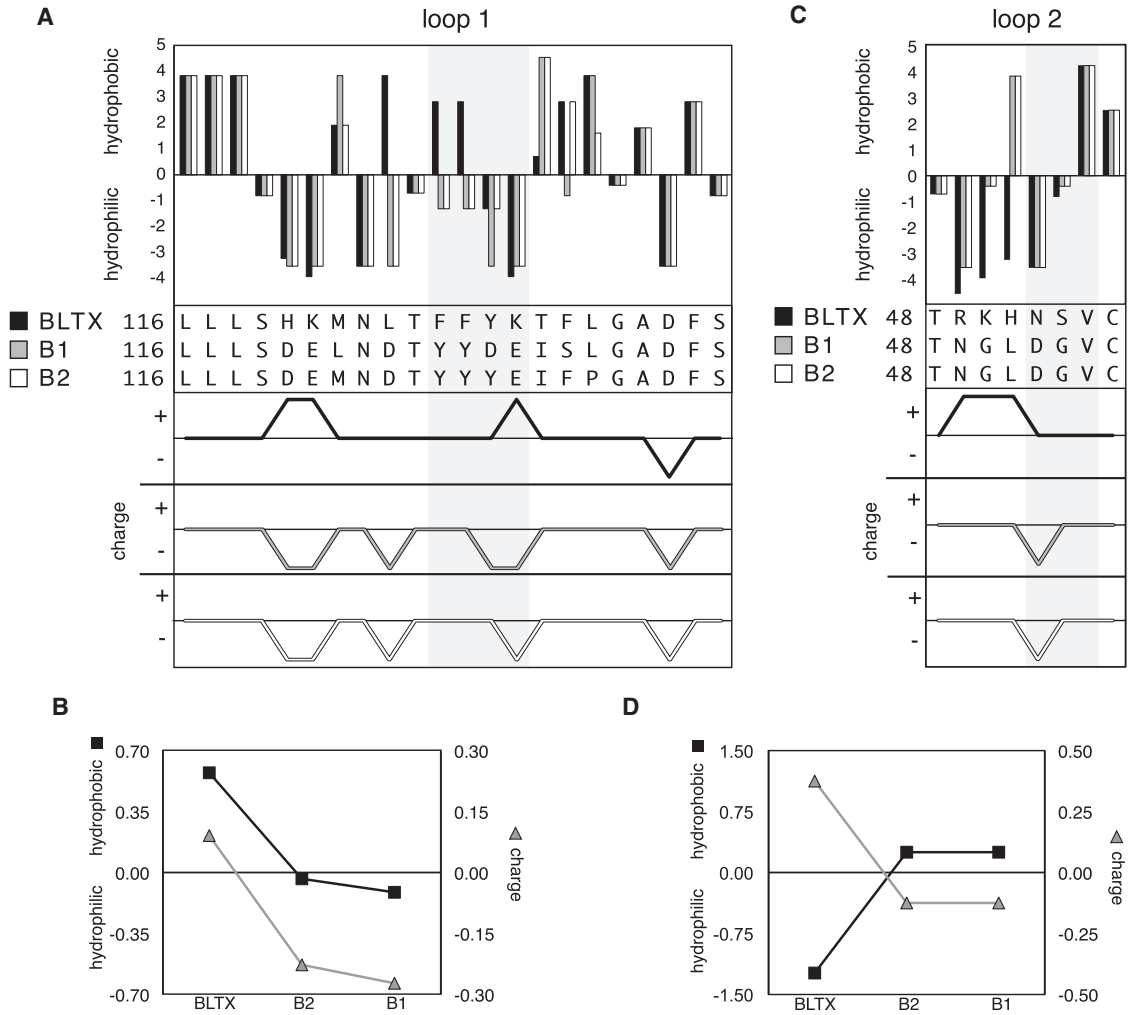

Figure 2. Physicochemical Pattern of Hydropathy and Charge in Loops 1 and 2 Correlates with Toxicity in BLTX

(A) For each amino acid residue in loop 1 (the kallikrein loop), hydropathy (top) and charge (bottom) are shown for BLTX (black), blarinasin-1 (gray), and blarinasin-2 (white). Charge was assigned as negative (−1) if Asp or Glu; positive (+1) if Lys, Arg, or His; and neutral (0) for all other amino acids.

(B) Average hydropathy and charge plotted for BLTX, B2, and B1.

(C) Hydropathy (top) and charge (bottom) shown for each amino acid in loop 2.

(D) Average hydropathy and charge plotted for BLTX, B2, and B1.

mutations share unique physicochemical properties. We quantified two properties of amino acids relevant to protein function—hydropathy and charge—for each of the residues in the five loops of BLTX, blarinasin-1, and blarinasin-2. Although we did not find any strong differences in the physicochemical properties among the three proteins in loops 3–5 (Table S2), BLTX shows a dramatic shift in both hydropathy and charge for both loop 1 and 2. Loop 1 is hydrophilic in both blarinasin-1 and -2, but is strongly hydrophobic in BLTX (Figure 2A). In addition, we found a difference in the average per residue charge in loop 1: BLTX has an equal or more positively charged amino acid at every site compared with blarinasin-1 and -2 (Figure 2A). The average per-residue charge value for BLTX is positive (+0.09), whereas that for blarinasin-1 and -2 is negative (−0.27 and −0.23, respectively). Similar analysis on loop 2 reveals it is hydrophobic for both blarinasin-1 and -2, whereas BLTX is strongly hydrophilic (Figure 2B). We also found a concomitant difference in loop 2 charge. Most strikingly, three sites that are neutrally charged in blarinasin-1 and -2 (N49-L51) are positive in BLTX (R49-H51), and the only charged site in blarinasin-1 and -2 loop 2 (D52) is neutral in BLTX (N52). The average per residue charge value for loop 2 in BLTX is strongly positive (+0.375), whereas that for blarinasin-1 and -2 is negative (−0.13). Thus, BLTX loops 1 and 2 have evolved distinct physicochemical properties from blarinasin-1 and -2: loop 1 is hydrophobic, loop 2 is strongly hydrophilic, and both are positively charged. Notably, physicochemical properties have changed only in the loops that acquired insertions.

Predicted Structural Changes Consistent with Increased Catalysis

To determine to what extent, if any, the acquisition of insertions and the novel physicochemical properties of the regulatory loops might result in topological changes that can lead to increased catalysis, we subjected 3D models of human KLK1 (hKLK1), BLTX, blarinasin-1, and blarinasin-2 to molecular dynamics (MD) simulations. Here, we report three distinct

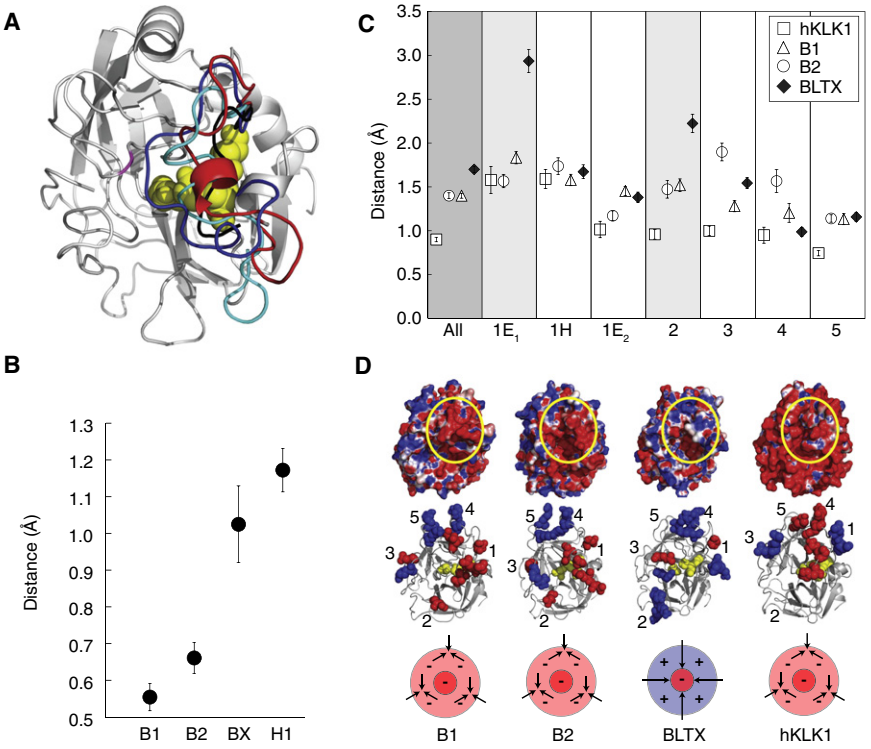

Figure 3. Predicted Structural Changes in BLTX, Blarinasin-1, Blarinasin-2, and Human Kallikrein-1

(A) Three-dimensional structures based on molecular dynamics simulations are aligned and oriented with the catalytic cleft in the foreground. Loop 1 in B1 (blue), B2 (cyan), BLTX (red), and human KLK1 (black) hover over the catalytic triad (yellow spheres) to different degrees. All four loop 1 conformations are shown on the BLTX model (gray).

(B) The distance (Å) between the tip of loop 5 (magenta in panel A) and loop 1 was calculated for B1, B2, BLTX, and human KLK1 (± standard deviation).

(C) Flexibility measurements for all five loops (dark gray shade), the first extension, helical region, and second extension regions of loop 1 ($1E_1$, 1H, and $1E_2$, respectively), and loops 2–5 individually in blarinasin-1, blarinasin-2, BLTX, and human kallikrein-1. Light gray shaded areas ($1E_1$, and loop 2) represent regions that differ in both length and polarity between BLTX and hKLK1, showing the most striking difference in flexibility. Each point is an average distance and error bars are standard errors.

(D) Electrostatic potential of the four proteins. Red denotes negative charge/potential and blue positive charge/potential. The top panel shows the surface electrostatic potential of the 3D protein models. Yellow circle demarks the active site (docking site is at its center). The middle panel highlights the contribution of the charged residues in regulatory loops 1–5 (shown as spheres) to the surface electrostatic potential around the active site. The catalytic triad is shown as yellow spheres. The bottom panel summarizes the simplified surface electrostatic potential and the active site charge of the four proteins, demonstrating how it can modulate accessibility of a positively charged substrate.

predicted structural changes to the BLTX active site that together probably lead to increased catalysis.

We first tested if substrate accessibility may be increased by a more exposed active site. Simulations reveal that loop 1 of BLTX has a more compressed conformation relative to blarinasin-1 and -2, exposing the active site (Figure 3A). To estimate the extent of active site occlusion by loop 1, we measured the distance between the tip of loop 5 (S253 in BLTX, Y252 in blarinasin-1 and -2) and the extended portion of loop 1 for each protein. We find that the active site opening is significantly larger in BLTX compared to blarinasin-1 and -2 (Figure 3B). Loop 1 in BLTX is further from the active site relative to blarinasin-1 and -2 by an average of 4.7 Å and 3.6 Å, respectively. The kallikrein loop has been shown to regulate accessibility to the active site [10], and therefore a more compressed conformation due to its increased hydrophobicity probably increases catalytic rate, as seen in other enzymes (e.g., [16]). However, the opening of the active site is not significantly different between BLTX and the nontoxic human KLK1 (Figure 3B), suggesting that active site accessibility alone is not sufficient to cause toxicity and other changes unique to BLTX are required.

Second, increased enzyme activity can also be modulated by a more flexible protein structure that allows for rapid conformational changes during catalysis [17]. Our simulations also show that BLTX's active site surface, as defined by the five regulatory loops, is significantly more flexible than blarinasin-1, blarinasin-2, and especially hKLK1 (Figure 3C). Average fluctuation per atom across regulatory loops is 1.7 Å for BLTX but only 0.9 Å for hKLK1 (Mann-Whitney $U_A = 222883$, $z = 16.06$, $p < 0.0001$). Specifically, the two regulatory loops with insertions show significant fluctuation relative to hKLK1: loop 1 of BLTX has an average fluctuation per atom of 2.9 Å relative to 1.2 Å of the homologous region in hKLK1, and loop 2 has 2.2 Å relative to 0.9 Å of hKLK1 (Figure 3B; Mann-Whitney $U_A = 296, 538$, $z = 4.48, 8.3$, $p < 0.0001$, respectively). Two features, the increased length and the polarity of the regulatory loops, might give rise to increased flexibility by improving solvent interactions and reducing the compactness of the molecule [18] as is indeed the case for BLTX relative to hKLK1 (Table S3).

Third, the charge distribution (e.g., surface electrostatic potential) surrounding the active site, relative to the substrate, is a third mechanism by which catalysis may be altered [19]. In BLTX, we find a dramatic shift toward a positive charge in the loops that surround the active site—four of the five regulatory loops (loops 1, 2, 4, and 5) are positively charged—which significantly alters the active site surface. In fact, although as much as 40% (12 of 30) of the positively charged residues in BLTX cluster within the five regulatory loops, only 8% (2 of 23) of the negatively charged residues are found in this region. The trend is opposite for blarinasin-1 and -2, with the active site surface holding only 21% (6 of 28) of the positively charged and 31% (9 of 29) of the negatively charged residues. To visualize the distribution of charged residues in the simulated 3D structures, we generated surface electrostatic potential maps for each protein. Both blarinasin-1 and -2 exhibit a predominantly negatively charged catalytic cleft (only loops 4 and 5 are positively charged) similar to hKLK1 (Figure 3C). By contrast, for BLTX, the catalytic cleft is predominantly positively charged, whereas the actual active site (at the center) is negatively charged (Figure 3C). Biochemical

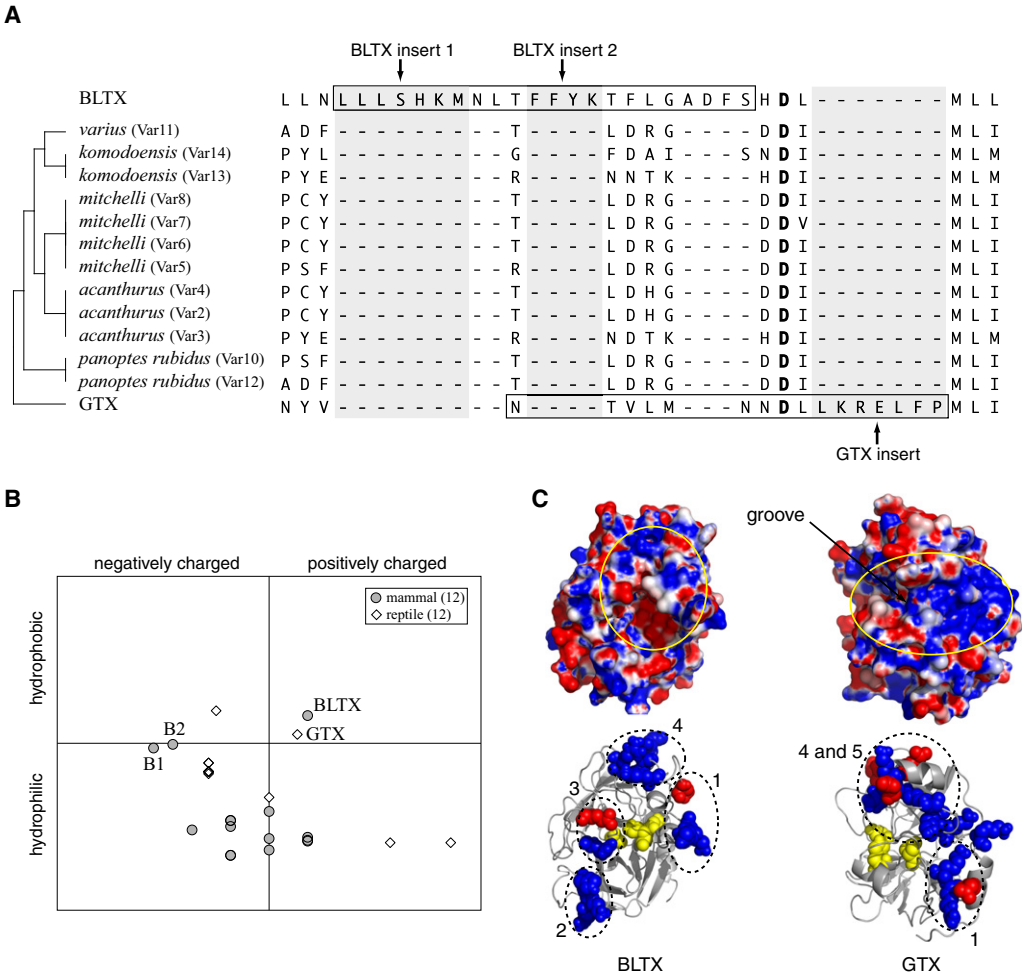

Figure 4. Convergent Evolution of Venom in Shrews and Lizards

(A) Sequence alignment of reptilian kallikrein-like proteins from 12 *Varanus* species and GTX from the venomous *Helodermata horridum*. Topology showing *Varanus* species relationships shown on left. Unique insertion in GTX of seven residues is labeled and highlighted in gray. The GTX insertion is downstream of the conserved catalytic aspartate (in bold) and the kallikrein loop in mammalian homologs (top box), and nonoverlapping with the two BLTX insertions (gray). The lizard insertion, along with upstream sequence excluding the conserved aspartate, forms an analogous regulatory loop to that found in mammalian kallikreins (bottom box).

(B) Comparison of the average hydropathy and charge of 12 mammalian (including B1 and B2) and 12 reptilian kallikrein loops to the two toxic enzymes (BLTX and GTX).

(C) Three-dimensional representations of the electrostatic potentials for BLTX and GTX in which red denotes negative charge/potential and blue positive charge/potential. Yellow circles highlight the active site (top panel). Cartoon representation in the same orientation highlights the contribution of the charged amino acid residues in the regulatory loops to surface potential. Loops are labeled with dashed circles (bottom panel). The catalytic triad is shown as yellow spheres.

characterization of BLTX has demonstrated a strong preference for substrates (both natural and artificially synthesized) that are positively charged at position 1 [1]; thus, a positively charged surface surrounding a negatively charge active site might serve to most efficiently direct the preferred substrate toward the active site. This contrast between the surface and active site charge thus might also contribute to BLTX's increased catalytic rate.

Convergent Evolution of BLTX and a Lizard Venom GTX

One way to link these molecular changes with a causal functional effect is to demonstrate convergent evolution in other kallikrein-like toxins. In other words, if the structural modifications and physicochemical characteristics of BLTX's catalytic cleft are important for the evolution of toxicity, then other toxic kallikreins [2, 20] might have evolved via similar changes. To test this prediction, we examined the evolution of the kallikrein-related serine protease GTX from the Mexican beaded lizard (*Heloderma horridum),* which is thought to confer toxicity by increased catalysis like BLTX [2]. First, like BLTX, GTX carries a unique 21 bp insertion immediately adjacent to loop 1 (just after the conserved aspartate, D96) [1]. We aligned GTX with 12 other lizard kallikrein-related proteins to demonstrate that the insertion is indeed unique to GTX (Figure 4A). Notably, this insertion is different from, but proximate to, the insertions found in loop 1 of BLTX. Second, GTX has also evolved a largely hydrophobic (+0.17) and positively charged (+0.07) loop 1 (defined as the original loop plus the seven inserted downstream residues excluding the conserved aspartate).

To confirm that these properties are unique to toxins, we performed similar physicochemical analysis for loop 1 in an additional 12 mammalian and 12 reptilian kallikrein proteins (Table S4), none of which are known to be toxic. We find that a hydrophobic and positively charged loop 1 is unique to BLTX and GTX (Figure 4B). Moreover, the physicochemical character of the GTX loop is similar to BLTX—the portion of the loop directly above the active site is hydrophobic and neutrally charged, but the inserted region, as in BLTX, is positively charged (Figure 4C). Thus, the loop 1 structure from two divergent toxic enzymes has independently increased in length (via short insertions) and evolved convergent physicochemical properties.

To determine whether these sequence changes in GTX result in changes in the 3D protein structure, we used MD simulations to model GTX. We first found that, similar to BLTX, the conformation of loop 1 promotes a more open active site; the distance between the tip of loop 5 and loop 1 in GTX is even larger (by an average of 3.5 Å) than that of BLTX. In addition, whereas in BLTX an increase in active-site exposure is achieved via a helical and more compressed loop 1 conformation (Figure 3A), in GTX increased exposure is due to a collapsed and linear loop conformation that minimizes hindrance of the active site by the loop (Figure 4C). Second, the active site surface of GTX is similar in flexibility to BLTX with an average fluctuation per atom across the loops of 1.4 ± 0.004 Å (Table S2) and an even higher fluctuation of loop 1 (1.9 ± 0.011 Å). Third, as in BLTX, surface electrostatic potential analysis shows that the unique GTX active site surface exhibits a trend similar to BLTX, with a distinct positively charged character around a negatively charged active site (Figure 4C). Thus, unlike any other kallikrein-like enzymes we examined, BLTX and GTX have evolved unique and similar characteristics.

Conclusions

We have shown that venom proteins from two diverged phyla, reptiles and mammals, have evolved independently from ancestral kallikrein-related serine proteases via similar structural modifications, which might lead to the similar degrees of toxicity of BLTX and GTX [1]. Parallel changes in the spatial and physicochemical properties, clustered in functionally important protein regions, also have been reported in the evolution of novel chimeric genes [21]. In both BLTX and GTX, novel insertions increase the length, and hence the conformation, of the regulatory loops that surround the active site. Amino acid mutations in these loops (and in the insertions) have also altered the physicochemical properties and topology of the active site, modifications that might increase substrate accessibility and hence catalysis in three ways: increased exposure of the active site, more flexibility in the regulatory loops, and a change in the surface electrostatic potential. Future functional studies will allow us to determine the individual effects of these mutations on enzyme activity.

How repetitive, and thus predictable, is evolution? This example of convergent molecular evolution of two kallikrein-like toxins from distant species, together with other examples from venom proteins in diverse lineages [3], suggests that adaptation may be highly predictable. As such, these common results might aid in the identification of other naturally occurring toxic proteins from diverse species. For example, a kallikrein-like enzyme (KR-E-1) was recently isolated from the viper *Agkistrodon caliginosus* [20], and the kallikrein loop of this enzyme is highly enriched for positively charged residues (particularly lysine residues), a characteristic associated with toxicity. Moreover, the convergent mechanisms for increased catalytic activity described here might be more universal and applicable to a broad range of enzymes, which have evolved changes in catalysis rate. For example, enzymes from cold adapted organisms have increased catalytic efficiency to compensate for slower function in low temperatures through mechanisms similar to those described here (e.g., [18, 19]). Thus, the combination of population-genetic analyses and protein modeling, together with previous biochemical studies [1], allowed us to identify convergent structural changes associated with the evolution of toxicity specifically, and with increased catalysis more generally.

Supplemental Data

Supplemental Data include Supplemental Experimental Procedures, four tables, and one figure and can be found with this article online at http://www.cell.com/current-biology/supplemental/S0960-9822(09)01701-1.

Acknowledgments

We would like to thank D. Jeruzalmi for guidance and assistance with MODELLER; N. Crawford, E. Kay, B. Peterson, and other members of the Hoekstra Lab for useful discussion; and D.A. Drummond, C. Extavour, A. Leschziner, D. Petrov, and two anonymous reviewers for comments on the manuscript. This work was supported by funds from the Federico Foundation and Harvard University.

Received: July 23, 2009
Revised: September 8, 2009
Accepted: September 14, 2009
Published online: October 29, 2009

References

1. Kita, M., Nakamura, Y., Okumura, Y., Ohdachi, S.D., Oba, Y., Yoshikuni, M., Kido, H., and Uemura, D. (2004). Blarina toxin, a mammalian lethal venom from the short-tailed shrew *Blarina brevicauda*: Isolation and characterization. Proc. Natl. Acad. Sci. USA *101*, 7542–7547.
2. Utaisincharoen, P., Mackessy, S.P., Miller, R.A., and Tu, A.T. (1993). Complete primary structure and biochemical properties of Gilatoxin, a serine protease with kallikrein-like and angiotensin-degrading activities. J. Biol. Chem. *268*, 21975–21983.
3. Fry, B.G., Roelants, K., and Norman, J.A. (2009). Tentacles of venom: Toxic protein convergence in the kingdom Animalia. J. Mol. Evol. *68*, 311–321.
4. Dufton, M.J. (1992). Venomous mammals. Pharmacol. Ther. *53*, 199–215.
5. Pucek, M. (1959). The effect of the venom of the European water shrew (*Neomys fodies fodies* Pennant) on certain experimental animals. Acta Theriol. (Warsz.) *3*, 93–104.
6. Pearson, O.P. (1942). On the cause and nature of a poisonous action produced by the bite of a shrew (*Blarina brevicauda*). J. Mammal. *23*, 159–166.
7. Martin, I.G. (1981). Venom of the short-tailed shrew (*Blarina brevicauda*) as an insect immobilizing agent. J. Mammal. *62*, 189–192.
8. Kita, M., Okumura, Y., Ohdachi, S.D., Oba, Y., Yoshikuni, M., Nakamura, Y., Kido, H., and Uemura, D. (2005). Purification and characterisation of blarinasin, a new tissue kallikrein-like protease from the short-tailed shrew *Blarina brevicauda*: Comparative studies with blarina toxin. Biol. Chem. *386*, 177–182.
9. Mason, A.J., Evans, B.A., Cox, D.R., Shine, J., and Richards, R.I. (1983). Structure of mouse kallikrein gene family suggests a role in specific processing of biologically active peptides. Nature *303*, 300–307.
10. Lundwall, A., and Brattsand, M. (2008). Kallikrein-related peptidases. Cell. Mol. Life Sci. *65*, 2019–2038.
11. Villoutreix, B.O., Getzoff, E.D., and Griffin, J.H. (1994). A structural model for the prostate disease marker, human prostate-specific antigen. Protein Sci. *3*, 2033–2044.
12. Bode, W., Chen, Z.G., Bartels, K., Kutzbach, C., Schmidtkastner, G., and Bartunik, H. (1983). Refined 2 A X-ray crystal structure of porcine

pancreatic kallikrein A, a specific trypsin-like seringe proteinase, crystallization, structure determination, crystallographic refinement, structure and its comparison with bovine trypsin. J. Mol. Biol. *164*, 237–282.

13. Carvalho, A.L., Sanz, L., Barettino, D., Romero, A., Calvete, J.J., and Romao, M.J. (2002). Crystal structure of a prostate kallikrein isolated from stallion seminal plasma: A homologue of human PSA. J. Mol. Biol. *322*, 325–337.
14. Polley, S.D., and Conway, D.J. (2001). Strong diversifying selection on domains of the *Plasmodium falciparum* apical membrane antigen 1 gene. Genetics *158*, 1505–1512.
15. Berglund, A.C., Wallner, B., Elofsson, A., and Liberles, D.A. (2005). Tertiary windowing to detect positive diversifying selection. J. Mol. Evol. *60*, 499–504.
16. Russell, R.J.M., Gerike, U., Danson, M.J., Hough, D.W., and Taylor, G.L. (1998). Structural adaptations of the cold-active citrate synthase from an Antarctic bacterium. Structure *6*, 351–361.
17. Gerday, C., Aittaleb, M., Bentahir, M., Chessa, J.-P., Claverie, P., Collins, T., D'Amico, S., Dumont, J., Garsoux, G., Georlette, D., et al. (2000). Cold-adapted enzymes: From fundamentals to biotechnology. Trends Biotechnol. *18*, 103–107.
18. Siddiqui, K.S., and Cavicchioli, R. (2006). Cold-adapted enzymes. Annu. Rev. Biochem. *75*, 403–433.
19. Moe, E., Leiros, I., Riise, E.K., Olufsen, M., Lanes, O., Smalås, A., and Willassen, N.P. (2004). Optimisation of the surface electrostatics as a strategy for cold adaptation of uracil-DNA *N*-glycosylase (UNG) from Atlantic cod (*Gadus morhua*). J. Mol. Biol. *343*, 1221–1230.
20. Oyama, E., Fukuda, T., and Takahashi, H. (2008). Amino acid sequence of a kinin-releasing enzyme, KR-E-1, from the venom of *Agkistrodon caliginosus* (Kankoku-mamushi). Toxicon *52*, 651–654.
21. Jones, C.D., and Begun, D.J. (2005). Parallel evolution of chimeric fusion genes. Proc. Natl. Acad. Sci. USA *102*, 11373–11378.
22. Nishihara, H., Hasegawa, M., and Okada, N. (2006). Pegasoferae, an unexpected mammalian clade revealed by tracking ancient retroposon insertions. Proc. Natl. Acad. Sci. USA *103*, 9929–9934.
23. Menez, R., Michel, S., Muller, B.H., Bossus, M., Ducancel, F., Jolivet-Reynaud, C., and Stura, E.A. (2008). Crystal structure of a ternary complex between human prostate-specific antigen, its substrate acyl intermediate and an activating antibody. J. Mol. Biol. *376*, 1021–1033.